Application of the ORCHIDEE global vegetation model to evaluate biomass and soil carbon stocks of Qinghai-Tibetan grasslands

Kun Tan, Philippe Ciais, Shilong Piao, Xiaopu Wu, Yanhong Tang, Nicolas Vuichard, Shuang Liang, Jingyun Fang

Application of the ORCHIDEE global vegetation model to evaluate biomass and soil carbon stocks of Qinghai-Tibetan grasslands

Kun Tan,[1] Philippe Ciais,[2] Shilong Piao,[1] Xiaopu Wu,[3] Yanhong Tang,[4] Nicolas Vuichard,[2] Shuang Liang,[1] and Jingyun Fang[1]

Received 27 March 2009; revised 8 October 2009; accepted 15 October 2009; published 20 March 2010.

[1] The cold grasslands of the Qinghai-Tibetan Plateau form a globally significant biome, which represents 6% of the world's grasslands and 44% of China's grasslands. Yet little is known about carbon cycling in this biome. In this study, we calibrated and applied a process-based ecosystem model called Organizing Carbon and Hydrology in Dynamic Ecosystems (ORCHIDEE) to estimate the C fluxes and stocks of these grasslands. First, the parameterizations of ORCHIDEE were improved and calibrated against multiple time-scale and spatial-scale observations of (1) eddy-covariance fluxes of CO_2 above one alpine meadow site; (2) soil temperature collocated with 30 meteorological stations; (3) satellite leaf area index (LAI) data collocated with the meteorological stations; and (4) soil organic carbon (SOC) density profiles from China's Second National Soil Survey. The extensive SOC survey data were used to extrapolate local fluxes to the entire grassland biome. After calibration, we show that ORCHIDEE can successfully capture the seasonal variation of net ecosystem exchange (NEE), as well as the LAI and SOC spatial distribution. We applied the calibrated model to estimate 0.3 Pg C yr^{-1} (1 Pg = 10^{15} g) of total annual net primary productivity (NPP), 0.4 Pg C of vegetation total biomass (aboveground and belowground), and 12 Pg C of SOC stocks for Qinghai-Tibetan grasslands covering an area of 1.4×10^6 km^2. The mean annual NPP, vegetation biomass, and soil carbon stocks decrease from the southeast to the northwest, along with precipitation gradients. Our results also suggest that in response to an increase of temperature by 2°C, approximately 10% of current SOC stocks in Qinghai-Tibetan grasslands could be lost, even though NPP increases by about 9%. This result implies that Qinghai-Tibetan grasslands may be a vulnerable component of the terrestrial carbon cycle to future climate warming.

Citation: Tan, K., P. Ciais, S. Piao, X. Wu, Y. Tang, N. Vuichard, S. Liang, and J. Fang (2010), Application of the ORCHIDEE global vegetation model to evaluate biomass and soil carbon stocks of Qinghai-Tibetan grasslands, *Global Biogeochem. Cycles*, *24*, GB1013, doi:10.1029/2009GB003530.

1. Introduction

[2] The Qinghai-Tibetan Plateau extends over 2.0×10^6 km^2 with an average altitude above 4000 m above sea level. It is the largest geomorphologic unit on the Eurasian continent, about 1.4 times the size of Alaska [*Li and Zhou*, 1998; *Zheng et al.*, 2000]. The regional climate is characterized by a short and cool growing season lasting from May to September. But during the growing season, the vegetation receives both high solar radiation and relatively high precipitation (Figure 1). The main vegetation of the plateau is grassland, which includes alpine meadow, alpine steppe and alpine meadow steppe [*Sun*, 1996]. The biome area is 1.39×10^6 km^2 [*Editorial Board of Vegetation Map of China, Chinese Academy of Sciences* (*EBVMC*), 2001], which is ~44% of the total grassland area of China [*EBVMC*, 2001] and 5.8% of the worldwide grassland area [*Scurlock and Hall*, 1998]. Qinghai-Tibetan grasslands are hence regionally dominant and globally significant for understanding the terrestrial carbon cycle. In addition, the Qinghai-Tibetan plateau is a very sensitive region to climate change. Over the last five decades, the temperature rose faster than in other regions at the same latitude [*Liu and Chen*, 2000]. This strong warming signal has been accompanied by a precipitation increase in most parts of the region [*Niu et al.*, 2004;

[1]Department of Ecology, College of Urban and Environmental Science, and Key Laboratory for Earth Surface Processes of the Ministry of Education, Peking University, Beijing, China.
[2]UMR CEA, LSCE, CNRS, Gif-sur-Yvette, France.
[3]Chinese Research Academy of Environmental Sciences, Beijing, China.
[4]National Institute for Environmental Studies, Tsukuba, Japan.

0886-6236/10/2009GB003530

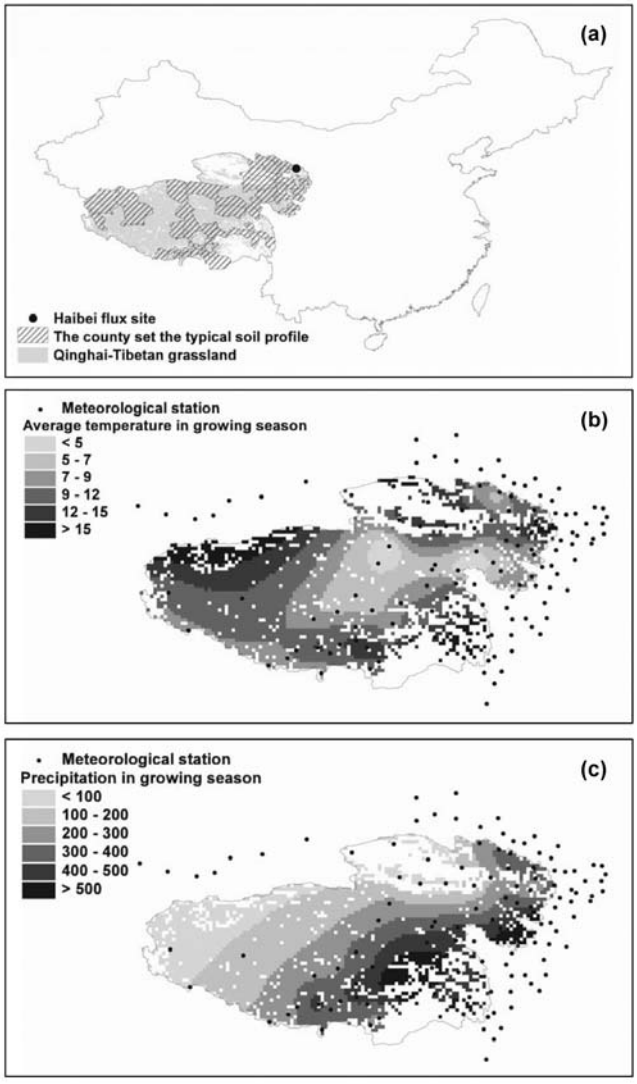

Figure 1. Spatial distribution of (a) grasslands, (b) average growing season temperature, and (c) growing season precipitation in the Qinghai-Tibetan Plateau. The 125 meteorological stations used to generate monthly climate data are also plotted in Figures 1b and 1c.

Liu et al., 2007]. *IPCC* [2007] reported that regional temperature will keep increasing in the future, under rising greenhouse gas concentrations forcing.

[3] This unique climate regime, coupled with a low intensity of human disturbance [*Li and Zhao*, 2001; *Wang et al.*, 2003] makes it important to quantify and understand current carbon fluxes and stocks, and their future evolution. *Kato et al.* [2004] measured CO_2 exchange at an alpine meadow site by eddy-covariance method. *Wang et al.* [2008] measured biomass and carbon stocks for Tibetan (excluding Qinghai) grasslands by traditional carbon density sampling methods, but their study failed to exhibit detailed and spatial biomass carbon stocks. Combined with ecosystem online flux measurements and inventory-based C stock surveys, process-based ecosystem models provide an effective method to estimate present-day regional C budgets and predict their future response to climate changes [*Sitch et al.*, 2007; *Piao et al.*, 2008, 2009]. *Zhang et al.* [2007] applied the CENTURY ecosystem model 4.5 version (http://www.nrel.colostate.edu/projects/century/) over the Qinghai-Tibetan grasslands. They investigated the spatiotemporal carbon dynamics of vegetation and soil by integrating the model at point locations (74 meteorological stations). The results were then interpolated to the whole plateau grassland area. This approach provides hints on coarse-scale gradients of carbon dynamics, but it does not allow precise geospatial estimation. *Piao et al.* [2006a] applied the Carnegie-Ames-Stanford Approach (CASA) model driven by remote sensing and climate fields, in order to evaluate the terrestrial net primary productivity (NPP) distribution over the Qinghai-Tibetan Plateau during 1982–1999. However, their results were not evaluated by observations, and thus should be viewed with caution.

[4] The primary objective of this paper is to quantify the state of the carbon cycle of the high-elevation Qinghai-Tibetan grassland biome and evaluate its response to future warming. To achieve this goal, the spatially explicit process-based model Organizing Carbon and Hydrology in Dynamic Ecosystems (ORCHIDEE) was applied. The model parameterizations were calibrated using four complementary data streams. First, eddy-covariance measurements at an alpine meadow site were used to constrain daily to seasonal gross primary productivity (GPP), terrestrial ecosystem respiration (TER), and net ecosystem exchange (NEE). Second, soil temperature measurements from 30 meteorological stations distributed across the Qinghai-Tibetan Plateau grasslands were used to validate the modeled soil thermal state, which in turns controlled soil respiration. Third, satellite-derived leaf area index (LAI) data collocated with 39 meteorological stations in Qinghai-Tibetan grasslands were used to validate the simulated phenology-climate relationships at regional scale. Finally, we used soil profile data from counties of the Qinghai-Tibetan Plateau sampled by China's Second National Soil Survey to validate the simulated soil carbon distribution. After the calibration procedure where parameters were adjusted to better reproduce the observations, the ORCHIDEE model was integrated wall-to-wall over the Qinghai-Tibetan grasslands (section 3.1). Based on the optimized model calculations, we assessed NPP and carbon stocks (section 3.2) as well as their changes in response to rising temperature by 2°C (section 3.3).

2. Data Sets and Methods

2.1. ORCHIDEE Model

[5] ORCHIDEE calculates the fluxes of CO_2, H_2O, and heat exchanged with the atmosphere on a 1/2-hourly basis, and of variations of water and carbon pools on a daily basis. The model is structured into two coupled modules [*Krinner et al.*, 2005]. The first module [*Ducoudré et al.*, 1993] describes the exchange of energy and water between the atmosphere and vegetation canopy, and the soil water budget with a time step of 30 min. The second module simulates the terrestrial carbon cycle including photosynthesis, respi-

ration, carbon allocation, litter decomposition, soil carbon dynamics, and phenology on a daily time step. In ORCHIDEE, the vegetation is described globally with 12 plant functional types (PFT). Each PFT follows the same set of governing equations but takes different parameters values, except for the leafy season onset and offset, which are defined by PFT-specific equations [*Krinner et al.*, 2005; *Piao et al.*, 2007a].

[6] Despite the complex processes described and their interactions (photosynthesis, surface energy budget, soil water balance, phenology, allocation, growth and mortality, litter and soil organic carbon (SOC) decomposition), the model has the advantage of requiring only generic climate drivers, available either at sites or on a grid [*Krinner et al.*, 2005]. It has been tested against eddy-covariance measurements across diverse biomes [*Krinner et al.*, 2005; *Santaren et al.*, 2007; *Jung et al.*, 2007] and proven to be well suited to study climate impacts on C balance [*Ciais et al.*, 2005; *Piao et al.*, 2008, 2009].

2.2. Data Sets

2.2.1. Eddy-Covariance Data

[7] The Haibei flux tower is located in an alpine meadow (latitude 37°36′N, longitude 101°18′E, elevation 3250 m; see Figure 1a), within the Haibei Research Station, Chinese Academy of Sciences [*Gu et al.*, 2003]. This meadow is dominated by *Kobresia humilis*, and the soil is a clay loam, with an average thickness of 65 cm, classified as Mat Crygelic Cambisols according to the Chinese national soil survey classification system [*Institute of Soil Science and the Chinese Academy of Sciences* (*ISSCAS*), 2001; *Gu et al.*, 2003; *Kato et al.*, 2004]. The annual precipitation and average temperature at the Haibei are 561 mm and −1.7°C for the period 1981–2000 [*Gu et al.*, 2003; *Kato et al.*, 2004]. Online CO_2 and water vapor fluxes were measured by an open-path eddy covariance system every 15 min during the period of 2002–2004, and corrected using Webb-Pearman-Leuning theory (WPL) density adjustments [*Webb et al.*, 1980; *Kato et al.*, 2006]. Detailed methods to separate fluxes of GPP and TER from NEE, and to fill gaps of missing values of these fluxes, including those at friction velocity $u^* < 0.2$ m s^{-1}, are reported by *Kato et al.* [2006]. In addition to carbon flux data, daily meteorology data sets, such as air temperature, rainfall, short-wave radiation, long-wave radiation, air humidity, atmospheric pressure, and wind speed, were also observed for the period of 2002–2004.

2.2.2. Satellite-Derived LAI Data Set

[8] Unfortunately, grassland leaf area index (LAI) was not measured at the flux tower location. It was obtained instead according to equation (1).

$$LAI = -1/k \times \ln(1 - FAPAR) \quad (1)$$

where Fraction of Absorbed Photosynthetic Active Radiation (FAPAR) was provided by European Commission–Joint Research Centre (EC-JRC) (http://fapar.jrc.ec.europa.eu/) from SeaWiFS at a resolution of 6 km/10 days from 2002 to 2004, with k the light extinction coefficient fixed to 0.5 [*Gobron et al.*, 2006]. In addition to EC-JRC data set, we also used Global Inventory Monitoring and Modeling Studies (GIMMS) LAI data with 0.25° resolution in 2001 (http://glcf.umiacs.umd.edu/data/gimms/) to validate our simulations. GIMMS LAI data were produced from satellite observations of normalized difference vegetation index (NDVI) using a three-dimensional radiative transfer model and a global land cover map [*Myneni et al.*, 1997; *Piao et al.*, 2006b]. The NDVI data are the GIMMS product of the NOAA/AVHRR series satellites [*Pinzon et al.*, 2005; *Tucker et al.*, 2005].

2.2.3. Soil Carbon Inventory Data

[9] China's Second National Soil Survey conducted from 1979 to 1985 consists of a database of 2473 typical soil profiles [*National Soil Survey Office*, 1993, 1994a, 1994b, 1995a, 1995b, 1996, 1998]. Each typical soil profile documents vegetation and soil type, county name of its geological location, soil depth, organic matter content, soil bulk density, soil texture, pH, and other soil physical and chemical properties. SOC density (SOCD, kg C m^{-2}) of each typical soil profile can be calculated by equation (2) [*Wu et al.*, 2003].

$$SOCD = \sum_{i=1}^{n} 0.58 \times SOM_i \times h_i \times BD_i \times (1 - C_i/100)/10 \quad (2)$$

where SOM_i, h_i, BD_i, and C_i represent soil organic carbon content (%), thickness (cm), bulk density (g cm^{-3}), and the fraction (%) of > 2 mm sand in a given soil layer i, respectively; and 0.58 is the Bemmelen constant converting SOM to SOC.

[10] We extracted from this data set soil carbon density measurements at 119 typical grassland soil profiles widely distributed over 51 counties of Qinghai-Tibetan (Figure 1a). The soil of Qinghai-Tibetan grassland is relatively shallow so that soil depth is mostly less than 100 cm, except in very limited meadow areas. Overall, nearly 90% of total SOC is concentrated in 0–50 cm soil layer, particularly in 0–30 cm layer with 70% of total SOC (Figure 2). Due to the lack of detailed geographical coordinate for each profile, we averaged the carbon density measurements of all the profiles within the same county to compare with the corresponding model-simulated grassland soil carbon densities for these counties.

2.2.4. Vegetation Distribution Information

[11] Information on the grassland distribution in the plateau was derived from the vegetation atlas of China [*EBVMC*, 2001] with a scale of 1:1,000,000. We used software Founder Mirage to digitize the atlas, and then extracted the Qinghai-Tibetan grass distribution from it (Figure 1a).

2.2.5. Climate Data

[12] Monthly air temperature, air temperature amplitude, precipitation, number of precipitation days, and air relative humidity data at 0.2° spatial resolution during the period of 1980–1990 were derived through interpolating observing climate data from 125 Chinese meteorological stations around Qinghai-Tibetan Plateau (39 of the stations are located over Qinghai-Tibetan grasslands), using kriging method (Figures 1b and 1c). The information on spatial distribution of monthly cloud cover and wind speed during the 1980s was supplied by the Climatic Research Unit, University of East Anglia, UK [*Mitchell and Jones*, 2005].

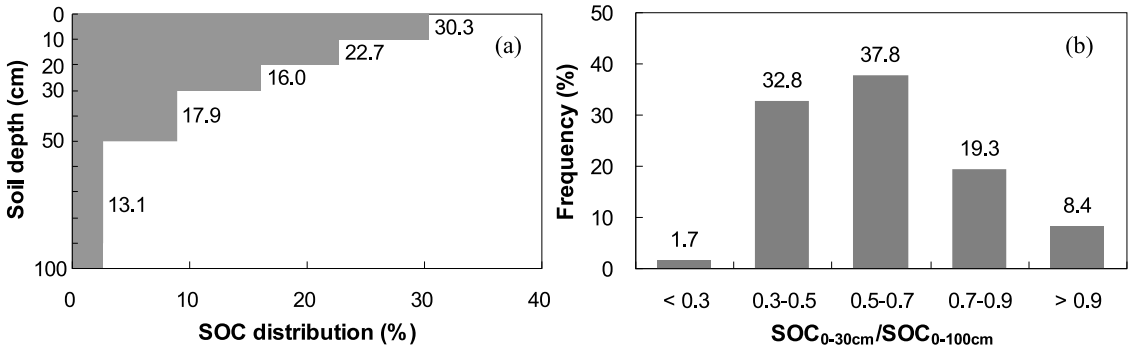

Figure 2. (a) Average soil organic carbon (SOC) vertical proportional distribution (0–10, 10–20, 20–30, 30–50, and 50–100 cm), and (b) frequency distribution of the proportion of SOC in 0–30 cm layer to total SOC of typical grassland soil profiles of Qinghai-Tibetan Plateau.

In addition, soil temperature at 20 cm depth observed across 30 of the meteorological stations at Qinghai-Tibetan grasslands for the period of 1980–1990 was also collected to validate ORCHIDEE modeled soil temperature.

2.3. ORCHIDEE Model Simulations

[13] For site-scale simulations at Haibei, we first ran the model until ecosystem carbon pools reached steady state equilibrium (long-term mean annual NEE $\approx$ 0), using the observed daily meteorology data sets (air temperature, rainfall, short-wave radiation, long-wave radiation, air humidity, atmospheric pressure, and wind speed) for 2002. Starting from this equilibrium state, the model was integrated for three years 2002–2004, forced by observed weather data.

[14] For regional simulations, using average monthly climate data with 0.2° spatial resolution during the period of 1980–1990, we brought ORCHIDEE into steady state with a spin-up of about 1000 years. The output of this simulation was then compared against observed soil temperature, LAI, and SOC observations, and the model parameterizations were optimized, where necessary. In order to further investigate the equilibrium response of grasslands to future climate change, we modeled the NPP and carbon stocks distribution under a +2°C warmer climate. This prescribed regional warming is at the lower range of the IPCC global projections of a 1.8–4.0°C warming by the end of the 21st century [*IPCC*, 2007]. To perform this climate change simulation, a new equilibrium state was calculated, forced by cycling current meteorological drivers, except that temperature was 2°C higher.

3. Results

3.1. Calibration of ORCHIDEE

[15] ORCHIDEE is an ecosystem model designed for global applications, and has never been applied for Qinghai-Tibetan grassland C balance diagnostic and analysis. The initial performances of the original model version Version-0 (V0) are not satisfactory (Figures 3 and 4). This implies that parameters calibration and/or model structural improvements are needed. The parameter calibration procedure, using site-scale eddy covariance C flux observations and regional-scale soil C inventories, is described below in three separate and incremental steps, leading to model versions V1 through V3 (Figure 3). These model versions have the same processes as V0, first with a spin-up to get steady state equilibrium for the ecosystem carbon pools.

3.1.1. Flux Controlling Parameters Improved From Eddy-Covariance Measurements

[16] Ecosystem gross GPP, TER fluxes, and absolute values of NEE are all overestimated in V0 (Figure 4). The simulated phenology lags the observation by roughly one month. The modeled leaf onset occurs too late and the initial LAI growth phase is too abrupt. Senescence is also sluggish and even never terminates during the late growing season (Figure 4). Given that any bias of GPP will strongly affect TER, and that the sum of these gross fluxes determines NEE, we choose to improve GPP and TER in order.

[17] First, we optimized biophysical canopy parameters. Observed attributes of Qinghai-Tibetan grasslands point to lower LAI, higher specific leaf area (SLA), shorter leaf age, and lower shoot/root ratio than the V0-version assigned parameter values. Unrealistic biophysical parameter values in V0 are suspected to be a primary source of the high bias of modeled GPP. According to field observations, we doubled SLA to 0.0288 m^2 (g C)$^{-1}$ [*He et al.*, 2006], shortened the critical leaf age from 180 days to 70 days [*Eckstein et al.*, 1999], and decreased the initial allocation of shoot/root ratio in growing season from 2/1 to 1/2 [*Hui and Jackson*, 2006].

[18] Then, in order to improve the leaf onset/offset phenology, we changed the critical functions to allow leaf development at a lower temperature and leaf senescence at a higher temperature. We decreased the growing degree-day critical threshold (*GDD_crit*) which depends on multiannual mean temperature *Tl* [*Botta et al.*, 2000; *Krinner et al.*, 2005] by 50°C × days (from $GDD\_crit = 270 + 6.25 \times Tl + 0.03125 \times Tl^2$ to $GDD\_crit = 220 + 6.25 \times Tl + 0.03125 \times Tl^2$). Leaf onset starts after actual *GDD* exceeds *GDD_crit*. We increased the senescence temperature threshold *T_crit* [*Krinner et al.*, 2005] by 7°C (from $T\_crit = -1.375 + 0.1 \times Tl + 0.00375 \times Tl^2$ to $T\_crit = 6.375 + 0.1 \times Tl + 0.00375 \times Tl^2$). Leaf turnover speeds up after actual temperature falls under *T_crit*, then leaf senescence would occur earlier. To avoid a too fast rise of GPP in the early growing season, as it is the case in V0, we constrained LAI

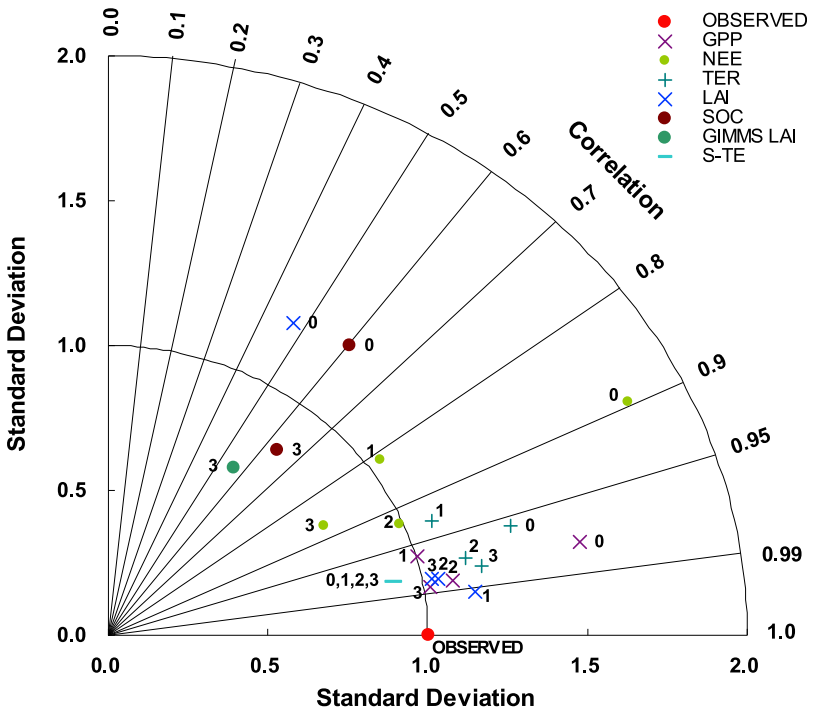

Figure 3. Second-order statistics of modeled and observed gross primary productivity (GPP), net ecosystem exchange (NEE), terrestrial ecosystem respiration (TER), and leaf area index (LAI) at Haibei site, average soil organic carbon density for 51 counties (SOC), LAI data at 39 meteorological stations (GIMMS LAI), and 20 cm depth soil temperature at 30 meteorological stations (S-TE). The radial coordinate gives the magnitude of total standard deviation (SD), normalized by the observed value, and the angular coordinate gives the correlation of simulations and observations. It follows that the distance between the OBSERVED point and any model's point is proportional to the centered root-mean-square (RMS) error, normalized by the observed SD Numbers indicate the model version.

to remain below 5% of LAI_{max} during the first 7 days of the growing season, instead of 50% of LAI_{max} during the first 14 days in the V0 version setup (LAI_{max} = prescribed yearly maximum LAI parameter). These parameters adjustments altogether defined a new model version called Version-1 (V1), calibrated to match the observed biophysical parameters and phenology.

[19] In the V1 version, GPP is realistically simulated, as a consequence of a seasonal cycle of LAI which is closer to observations. This implies that the resource use efficiency calculated by ORCHIDEE was probably correct in the initial V0 parameterization, so that an improved LAI dynamics alone is sufficient to match the observed GPP. It can be seen for instance that GPP in V1 shows a smoother increase during the first half of the growing season (Figure 4a), and that the phasing of simulated GPP and LAI is much closer to observed (Figure 3). The set of model modifications in V1, which targeted improvements of LAI, also has the positive effect of decreasing mean TER. Yet, TER can be seen to remain overestimated in V1 (Figure 4c), a bias which in turn makes the absolute value of NEE uptake too small (Figure 4b). In particular, simulated TER is positive during the nongrowing season (November–March; mean TER = 0.7 g C d^{-1} m^{-2}) unlike in the observations showing TER ≈ 0.

[20] To correct for this shortcoming, we modified the respiration sensitivity to temperature $f(T)$ by increasing the *Q10* parameter, which controls the SOM decomposition response to temperature. The *Q10* parameter was increased from *Q10* = 2 in Version V0 to *Q10* equal to 3 according to the observation of *Peng et al.* [2009], which gives:

$$f(T) = \exp[\ln(Q10) \times (T - 30°C)/10°C] \quad (3)$$

[21] This higher *Q10* value at lower temperatures defines a new model version, called Version-2 (V2). In V2, a reasonable agreement with the observed TER is found, and subsequently a more realistic NEE seasonal phase and amplitude (Figures 4b and 4c). The NEE model-data correlation coefficient is higher and centered root-mean-square (RMS) difference lower in V2 than in V1, showing a clear model improvement (Figure 3). Remark that the mean annual NEE flux is about 0, which is different from observed, because the grassland was assumed to be in equilibrium state in the model (section 2.3).

3.1.2. Evaluation Against in Situ Soil Temperature Data

[22] Soil temperature is a key determinant of soil respiration, so it is necessary to ensure that ORCHIDEE can simulate soil temperature well. The soil thermal module of ORCHIDEE calculates temperature from the surface down to 3 m depth, discretized with 7 layers. We used time series

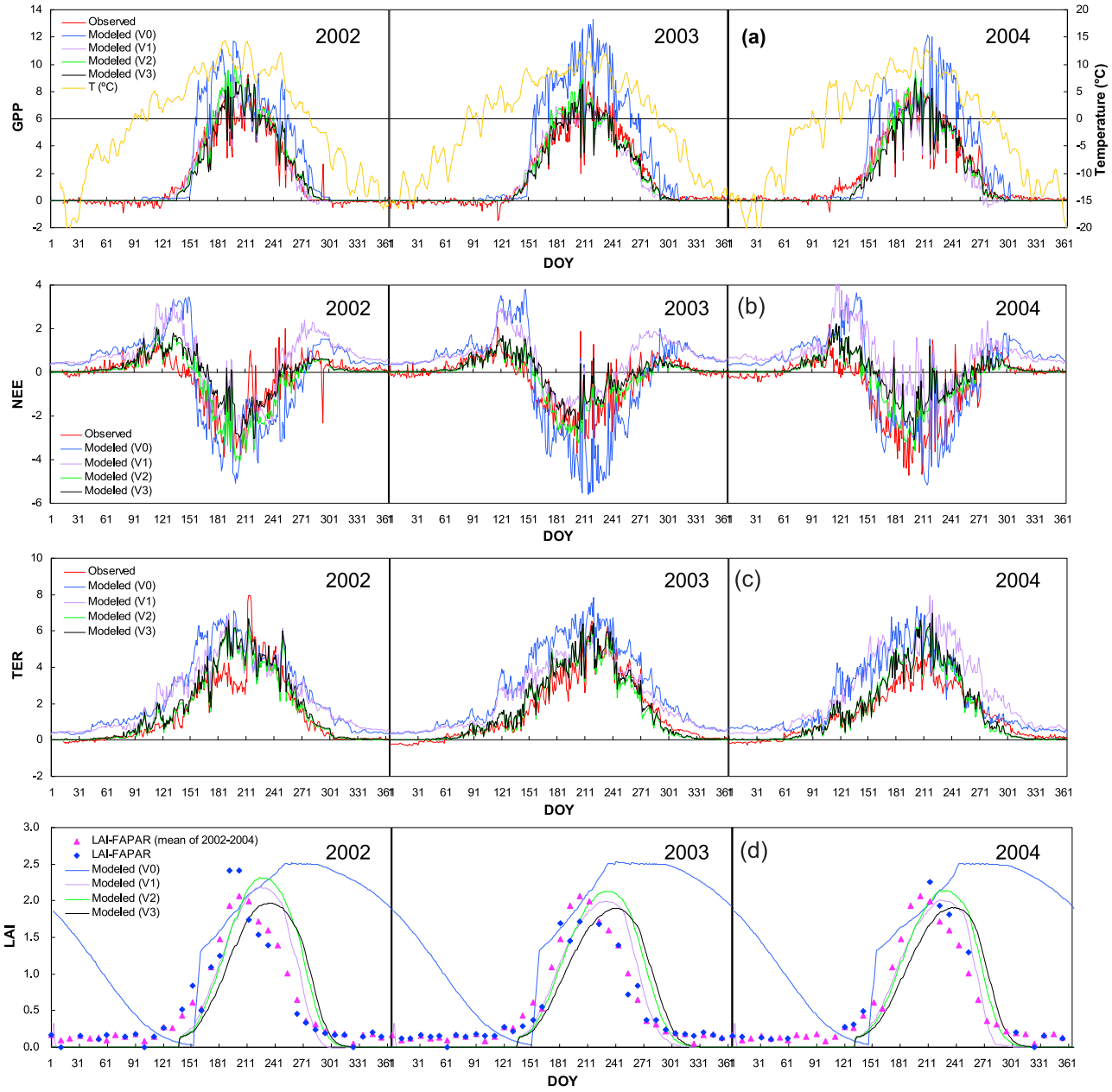

Figure 4. Comparisons of observed and modeled (a) GPP (g C d^{-1} m^{-2}), (b) NEE (g C d^{-1} m^{-2}), (c) TER (g C d^{-1} m^{-2}), and (d) LAI by the version of V0, V1, V2, and V3. Temperature in Figure 4a is 5 day moving average daily temperature.

of 20 cm depth soil temperature from 30 meteorological stations to evaluate the model. In this case, the model was forced locally by observed meteorological data. As shown in Figure 5, the simulation of shallow depth soil temperature is comparable with the observation, with annual RMSE of 1.56°C, but the modeled temperature is a little cooler in summer than observed, with spring, summer, autumn, and winter RMSE of 1.53°C, 2.29°C, 1.55°C, and 1.67°C, respectively.

3.1.3. Evaluation Against Satellite LAI Observations

[23] We integrated ORCHIDEE at all 39 meteorological stations forced by observed climate data, and simulated LAI as a proxy of vegetation activity. The LAI of Qinghai-Tibetan grasslands reaches its maximum in July or August, when aboveground biomass and total biomass are the highest. We thus compared the average of July–August simulated LAI with the NOAA-AVHRR GIMMS product and the SeaWiFS FAPAR product for year 2001. The RMSE between modeled and GIMMS-LAI is high (Figure 6). Nevertheless, modeled and observed LAI are distributed around the 1:1 line. One possible explanation for the low correlation is that the 0.25° resolution of the GIMMS data is too coarse to be compared to our point-scale simulations. We also note that the (spatial) range of LAI is small (0.5

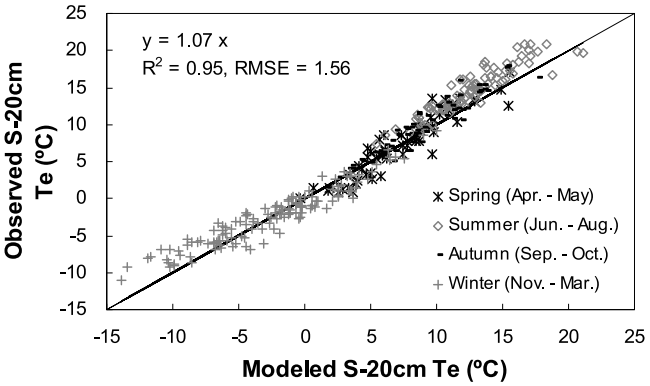

Figure 5. Comparisons of modeled and observed average monthly 20 cm depth soil temperature (S-20 cm Te) at 30 stations in Qinghai-Tibetan grasslands for 1980–1990.

to 2) which increases the noise. Comparison with the SeaWiFS observations is slightly better, as shown by Figure 6. The fact that the biases of NOAA-AVHRR and SeaWiFS satellite products are highly correlated between both sensors (Figure 6) suggests a common source of error in their comparison with point-scale simulation.

3.1.4. Soil Carbon Stock Validation

[24] Soil carbon stocks reflect C inputs and decomposition, and pedogenesis, accumulated over hundreds of thousands of years. Their spatial distribution is influenced not only by litter input (related to NPP), but also by decomposition and by processes not described in ORCHIDEE, such as wind and hydraulic erosion, DOC and DIC losses to river [*Chapin et al.*, 2002], and human disturbances (very low in that region). In the initial model version V0, the mean soil carbon density was 1.4 times larger than the soil database value (Figure 7a). Given that the seasonal cycle of NEE and

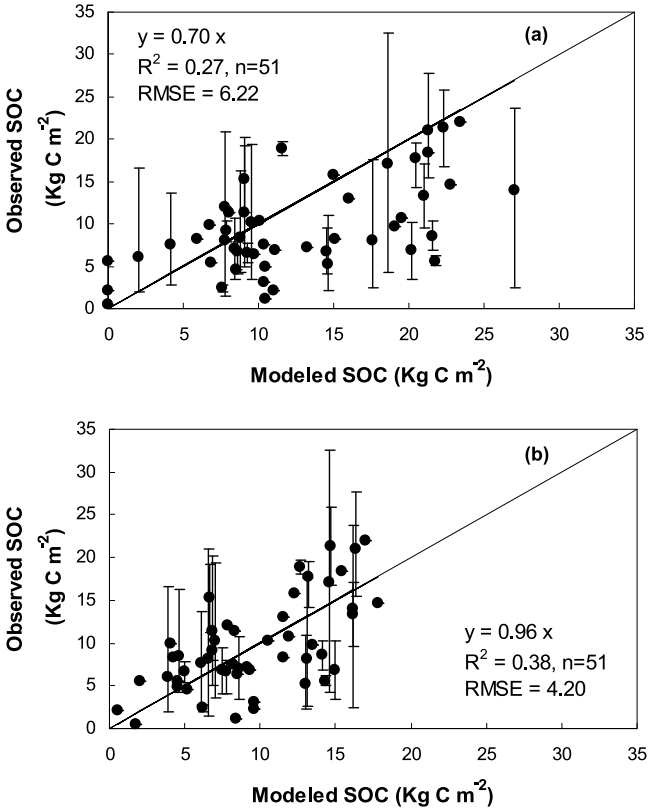

Figure 7. Comparisons of observed and modeled average grassland SOC density by the (a) initial version V0 and (b) final version V3 for 51 counties in Qinghai-Tibetan. The error bar shows minimum or maximum SOC density in the soil profiles.

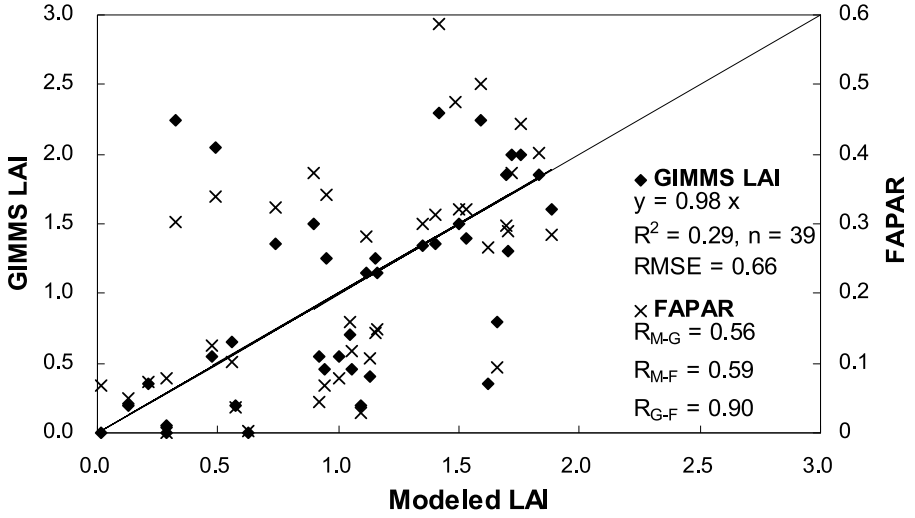

Figure 6. Relationship of average July and August LAI derived from ORCHIDEE model V3 with corresponding GIMMS LAI and FAPAR across 39 meteorological stations in Qinghai-Tibetan grasslands. R_{M-G}, R_{M-F}, and R_{G-F} represent correlation coefficient of modeled LAI and GIMMS LAI, modeled LAI and FAPAR, and GIMMS LAI and FAPAR, respectively.

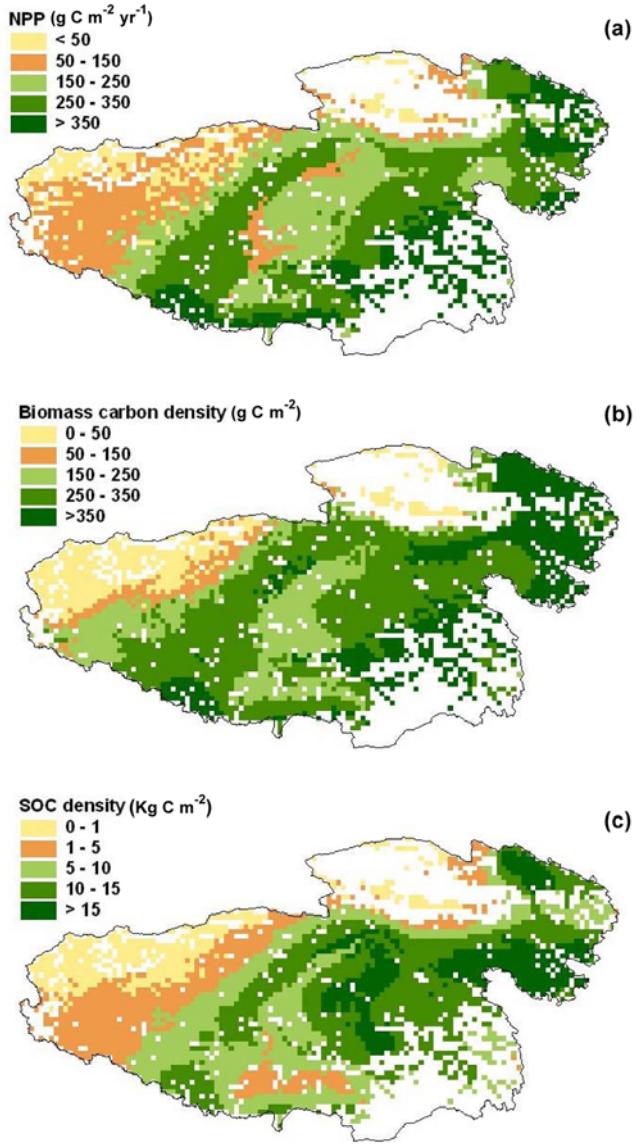

Figure 8. Spatial distributions of (a) annual net primary productivity (NPP), (b) total biomass carbon density, and (c) SOC density of Qinghai-Tibetan grasslands.

TER is simulated correctly at the Haibei site by the model version V2 (Figure 4), we assumed that the litter input flux was reasonable, and tuned the decomposition rates parameters in order to fit the observed soil C stocks. Here, we decreased the turnover time of passive soil carbon from 350 year to 70 years. Based on the previous estimates of 0.16 Pg C yr^{-1} in annual NPP [*Piao et al.*, 2006a], 0.35 Pg C in biomass stocks [*Piao et al.*, 2007a], and 7.4 Pg C in SOC stocks [*Yang et al.*, 2008] of Qinghai-Tibetan grasslands, one can estimate that the average turnover times for the whole Plateau grassland carbon stocks is about 48 yr, which is comparable to the results derived from V3 simulation (40 years). Doing so decreases the simulated SOC density and brings it closer to the observation (Figure 7b). The "soil optimized" model version, incremental to changes made in versions V1 and V2, is called V3. We checked for consistency that between V2 and V3, the modeled seasonal cycle of TER at Haibei is equally as well in agreement with the eddy-covariance measurements (Figures 3 and 4c).

3.2. Evaluation of NPP and Carbon Stocks of Qinghai-Tibetan Grasslands

[25] After the model "optimization" detailed in section 3.1, yielding to the development of version V3, we applied this version of ORCHIDEE on grids over the Qinghai-Tibetan grasslands, according to the protocol of section 2.3. The mean annual NPP of Qinghai-Tibetan grasslands (area = 1.39×10^6 km^2) is of 233 g C m^{-2} yr^{-1} over the period 1980–1990. About 60% of the regional grasslands have an annual NPP in the range 150–350 g C m^{-2} yr^{-1}. The southeast and the northwestern most part of the domain correspond to the highest and to the lowest annual NPP values, respectively (Figure 8a).

[26] The mean grasslands biomass C density is estimated to be 259 ± 117 g C m^{-2}, partitioned between 53.9 ± 27.7 g C m^{-2} aboveground and 205 ± 91 g C m^{-2} belowground. The spatial distribution of biomass C stocks is analogous to that of NPP, with highest values in southeastern regions, and lowest values in the northwestern part of the plateau (Figure 8b). The soil C stocks of the Qinghai-Tibetan plateau grasslands are 11.94 Pg C, with an average soil carbon density of 8.6 kg C m^{-2}. Roughly 75% of grasslands soils have a carbon density of 1–15 kg C m^{-2}, and 30% take a value of 10–15 kg C m^{-2} (Figure 8c).

[27] As shown by Figure 8, the spatial distribution of NPP, biomass and subsequent soil C stocks are rather similar to each other, with a negative gradient from the southeast to the northwest. These patterns are controlled by the interplay between temperature and precipitation controls (Figures 1b and 1c). The spatial correlation between NPP and biomass is high, as expected for annual plants ($R_{NPP\text{-}Biomass}$ = 0.88 for aboveground biomass and R = 0.83 for belowground biomass). The spatial correlation between soil C and NPP is smaller (R = 0.69), even though there is a well-defined linear relationship between soil C and NPP, as theoretically expected for the steady state solution of a set of first-order linear decay equations [*Wutzler and Reichstein*, 2008]. The scatter around the NPP versus soil C linear relationship is explained (in the model) by the different controls of temperature and rainfall on NPP (input) and on soil C decomposition rates.

3.3. Change in NPP and Carbon Stocks in Response to Rising Temperature by 2°C

[28] Figure 9 shows the projected changes of NPP, biomass, and SOC under a new future equilibrium climate with temperature higher than today by 2°C. As shown by Figure 9a, an increase in NPP is predicted in the southeastern part of the plateau where relatively high precipitation prevails. In contrast, a decrease of NPP is predicted in the dryer western part, where growing season precipitation is below 300 mm and growing season temperature higher than 10°C. The lower future NPP in the western part is likely to be

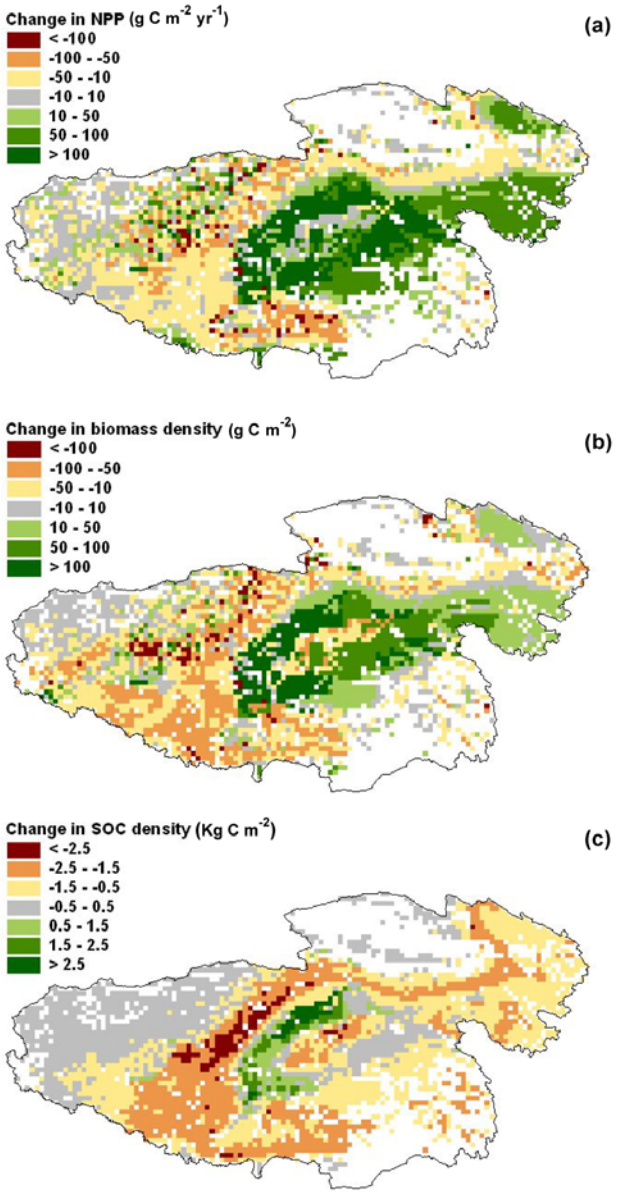

Figure 9. Spatial distributions of (a) the change in annual NPP, (b) total biomass carbon density, and (c) SOC density of Qinghai-Tibetan grasslands under the scenario of a 2°C increase in temperature.

related to the soil moisture stress driven by higher temperature. Overall, at the regional scale, a 2°C temperature increase will cause an 8.7% increase of NPP. Biomass C stocks (Figure 9b) changes follow a similar spatial pattern to NPP changes. The total biomass C stock for the entire region, however, does not change.

[29] In contrast to increase in NPP and biomass, more than 65% of the regions show a net decrease in soil C storage (Figure 9c). The largest soil C loss in response to warming occurs over the midwestern plateau where more than 20% of soil C stocks decrease under a 2°C warmer climate. At the regional scale, it is about 1.2 Pg of soil C that will be lost in 2°C warmer world, which is approximately 10% of today's stock.

4. Discussion

[30] Several modeling studies have investigated the spatiotemporal patterns of NPP and C stocks of the Qinghai-Tibetan Plateau. But very few studies tried to validate model output against observations, due to limited field and ground observations. Recently, *Piao et al.* [2006a] used the CASA model driven by satellite data to diagnose a mean NPP of 0.16 Pg C yr^{-1}. This satellite-driven NPP estimate represents only half of the process-modeled value of this study (0.32 Pg C yr^{-1}; area = 1.3×10^6 km^2 in the work of *Piao et al.* [2006a] and 1.4×10^6 km^2 in this study; see Table 1). A rather low NPP (0.13 Pg C yr^{-1}) was also estimated by *Zhang et al.* [2007]. However, the ratio of aboveground to belowground NPP used by *Zhang et al.* [2007] is 0.54, which is much higher than observed [*Hui and Jackson*, 2006]. We obtained a biomass C pool of 0.36 Pg C, which is consistent with the results of *Piao et al.* [2007a] (0.35 Pg C using statistical regression between site-scale field data and NDVI) (Table 1). For the total soil C pool, our estimation (11.94 Pg C) is larger than the one of *Yang et al.* [2008] (7.4 Pg C) and *Zhang et al.* [2007] (9.72 Pg C) (Table 1). It should be noted that, however, the results of *Zhang et al.* [2007] were obtained for surface organic carbon stocks at the depth of 0–20 cm. Considering that the proportion of SOC at 0–30 cm to that at 0–100 cm is 0.39–0.60 for steppe and meadow [*Yang et al.*, 2007], the *Zhang et al.* [2007] estimate extrapolated to 0–100 cm depth would be higher than our estimate.

[31] The total biomass carbon stocks of grasslands in China being about 1.05 Pg C [*Piao et al.*, 2007a] indicates that the Qinghai-Tibetan grasslands alone account for 34.3% of the whole-country grasslands biomass. Considering that Qinghai-Tibetan grasslands occupy 44% of total country grassland area, the average biomass carbon density of Qinghai-Tibetan grasslands is lower than in the rest of the country. Such relatively low biomass values are primarily driven by regionally lower temperatures. On the other hand, *Wu et al.* [2003] estimated the total SOC stock of China's grasslands to be 20–24 Pg C, of which Qinghai-Tibetan grasslands account for 50–60%. This means that, unlike biomass which is lower, the average SOC density is 13–36% higher than the mean of the country. Higher SOC is certainly related to slower decomposition due to lower temperature, which offsets lower inputs to the soil. As shown by Figure 1b, the mean growing season temperature over most of the Plateau is lower than 10°C. Furthermore, the biomass and soil C density of Qinghai-Tibetan grasslands is about two times lower than in Arctic tundra, which grow under a similar short and cold growing season (based upon biomass and SOC density of Arctic tundra of 700 g C m^{-2} and 22 kg C m^{-2}, reported by *Post et al.* [1982] and *Adams et al.* [1990]).

[32] Grasslands in Qinghai-Tibetan Plateau are suspected to be very sensitive to climate change, particularly to rising temperature [*Kato et al.*, 2004], but the evidence for this is very limited. Our simple (equilibrium) simulation under a 2°C

Table 1. Different Studies Estimated Grassland NPP, Biomass, and SOC in the Qinghai-Tibetan and the Tibetan[a]

		NPP		Biomass		SOC		
Region	Area (10^6 km^2)	Total (Pg C yr^{-1})	Density (g C m^{-2} yr^{-1})	Total (Pg C)	Density (g C m^{-2})	Total (Pg C)	Density (kg C m^{-2})	Source
Q-T	1.24			0.35	282			*Piao et al.* [2007a]
Q-T	1.31	0.16	122					*Piao et al.* [2006a]
Q-T	1.48	0.13	90			9.72[b]	6.6[b]	*Zhang et al.* [2007]
Q-T	1.14					7.40	6.5	*Yang et al.* [2008]
Q-T	1.39	0.32	233	0.36	259	11.94	8.6	This study
T	0.82			0.19	231			*Wang et al.* [2008]
T	0.89			0.20	230			This study

[a]Q-T, Qinghai-Tibetan; T, Tibetan (excluding Qinghai). NPP, net primary productivity.
[b]Soil organic carbon (SOC) only at the soil surface with the depth of 0–20 cm.

warmer temperature shows an increase in total GPP and NPP for Qinghai-Tibetan grasslands by 12% and 8.7%, respectively, implying that at the regional scale, future warming will benefit vegetation growth. Such an increase in vegetation productivity may be related to lengthening vegetation growing season [*Piao et al.*, 2007b]. Our simulation results indicate that the growing season is extended by one month with rising temperature of 2°C. The increase of vegetation productivity, however, does not lead to increase in SOC storage, even though a significant present-day positive spatial correlation between SOC and NPP or biomass density was modeled (Figure 8). The change in SOC is dependent on the balance between the increased amount of litter returning to the soil and the increased C losses from decomposition that are generally stimulated by rising temperature [*Davidson and Janssens*, 2006]. Our results suggest that 2°C of rising temperature causes an average increase of annual heterotrophic respiration by 11% during the first 100 years. As a result, in response to temperature increase of 2°C, the SOC pool of Qinghai-Tibetan grasslands decrease from 12 Pg C to 10.8 Pg C, i.e., a drop by 10%. This total C loss, of which 87% will occur over the first 100 years, would represent an extra 0.15% of the anthropogenic CO_2 emissions (7 Pg C yr^{-1}) released to the atmosphere by fossil fuel combustion and land use changes in a century [*IPCC*, 2007], and thus would provide a positive feedback to the global increase of atmospheric CO_2 and climate warming.

[33] Despite its decrease as a whole, SOC density in Qinghai-Tibetan plateau exhibits a pronounced geographical heterogeneity in its trends (Figure 9c), probably due to difference in climatic conditions. The increase in SOC density mainly occurs in areas with low growing season temperature but relatively high precipitation amount (200–400 mm; see Figures 1 and 9) over the Plateau. Accordingly in these regions, temperature may be the primary dominant limiting factor for vegetation growth, and rising temperature will significantly increase vegetation productivity (Figure 9a), thus enhance accumulation of SOC stocks. On the other hand, in the regions where growing season precipitation is less than 100 mm (Figures 1 and 9), 2°C of rising temperature causes decrease in biomass more than that in SOC due to the inhibited SOC decomposition driven by low soil moisture.

[34] Obviously, there are large uncertainties in our estimation of the state of the carbon cycle of the Qinghai-Tibetan grasslands. A first uncertainty lies in our assumption that this ecosystem is close to equilibrium, for it is out of our present knowledge whether grasslands ecosystems reach equilibrium state or not. The second uncertainty arises from the gridded climate forcing obtained by kriging meteorological stations data. One particular shortcoming is the network of meteorological stations being too sparse in the northwest part of the Plateau. Any bias of forcing will however have little effect on the simulated regional C balance, because the undersampled northwestern area (high elevation and dry/severe climate) is covered with sparse vegetation that has very low NPP and soil carbon stocks. A model error in that region would thus barely affect our whole-Plateau total carbon stock estimate. Third, our current modeling framework neglects human disturbances and grazing influences, as well as SOC erosion, due to lack of adequate information. Future inclusion of these processes will certainly improve our understanding of the C cycle over that region.

5. Conclusion

[35] The ORCHIDEE process-based ecosystem model, has been optimized to simulate NPP, biomass, and soil carbon stocks of the Qinghai-Tibetan grasslands. The optimization was done in three steps of parameter tuning. The optimized model is better able to reproduce the seasonality of NEE at one flux tower site, the seasonal cycle of soil temperature, and the spatial distribution of satellite-LAI observation and soil carbon density from inventories. This model-data fusion exercise not only suggests that a generic model like ORCHIDEE has great potential for simulating regional details of the C cycle of the Qinghai-Tibetan grasslands, but it also highlights the necessity of validation data on multiple temporal and spatial scales, to be able to constrain a global model for regional applications. In addition, the optimized model was applied under a warmer equilibrium climate, suggesting that future climate warming may cause in that region a significant decrease in total C storage. More research is needed to investigate the detailed spatio-temporal pattern of climate impacts on the Qinghai-Tibetan grasslands, and to formulate adaptation strategies.

[36] **Acknowledgments.** The authors wish to thank James Randerson and two anonymous referees for the detailed and constructive comments and Charlie Koven for checking English writing. This study was supported by the National Natural Science Foundation of China (grants 30970511 and

30721140306) and Foundation for the Author of National Excellent Doctoral Dissertation of PR China (FANEDD-200737).

References

Adams, J. M., H. Faure, L. Faure-Denard, J. M. McGlade, and F. I. Woodward (1990), Increases in terrestrial carbon storage from the Last Glacial Maximum to the present, *Nature*, *348*, 711–714, doi:10.1038/348711a0.

Botta, A., N. Viovy, P. Ciais, and P. Friedlingstein (2000), A global prognostic scheme of leaf onset using satellite data, *Global Change Biol.*, *6*, 709–726, doi:10.1046/j.1365-2486.2000.00362.x.

Chapin, F. S., III, P. A. Matson, and H. Mooney (2002), *Principles of Terrestrial Ecosystem Ecology*, pp. 50–53, Springer, New York.

Ciais, P., et al. (2005), Europe-wide reduction in primary productivity caused by the heat and drought in 2003, *Nature*, *437*, 529–533, doi:10.1038/nature03972.

Davidson, E. A., and I. A. Janssens (2006), Temperature sensitivity of soil carbon decomposition and feedbacks to climate change, *Nature*, *440*, 165–173, doi:10.1038/nature04514.

Ducoudré, N. I., K. Laval, and A. Perrier (1993), SECHIBA, a new set of parameterizations of the hydrologic exchanges at the land-atmosphere interface within the LMD atmospheric general circulation model, *J. Clim.*, *6*, 248–273, doi:10.1175/1520-0442(1993)006<0248:SANSOP>2.0.CO;2.

Eckstein, R. L., P. S. Karlsson, and M. Weih (1999), Leaf life span and nutrient resorption as determinants of plant nutrient conservation in temperate-Arctic regions, *New Phytol.*, *143*, 177–189, doi:10.1046/j.1469-8137.1999.00429.x.

Editorial Board of Vegetation Map of China, Chinese Academy of Sciences (EBVMC) (2001), *Vegetation Atlas of China*, Science Press, Beijing.

Gobron, N., et al. (2006), Evaluation FAPAR products for different canopy radiation transfer regimes: Methodology and results using JRC products derived from SeaWiFS against ground-based estimations, *J. Geophys. Res.*, *111*, D13110, doi:10.1029/2005JD006511.

Gu, S., Y. Tang, M. Du, T. Kato, Y. Li, X. Cui, and X. Zhao (2003), Short-term variation of CO_2 flux in relation to environmental controls in an alpine meadow on the Qinghai-Tibetan Plateau, *J. Geophys. Res.*, *108* (D21), 4670, doi:10.1029/2003JD003584.

He, J., Z. Wang, X. Wang, B. Schmid, W. Zuo, M. Zhou, C. Zheng, M. Wang, and J. Fang (2006), A test of the generality of leaf trait relationships on the Tibetan Plateau, *New Phytol.*, *170*, 835–848, doi:10.1111/j.1469-8137.2006.01704.x.

Hui, D., and R. B. Jackson (2006), Geographic and interannual variability in biomass partitioning in grassland ecosystems: A synthesis of field data, *New Phytol.*, *169*, 85–93, doi:10.1111/j.1469-8137.2005.01569.x.

Institute of Soil Science and the Chinese Academy of Sciences (ISSCAS) (2001), *Chinese Soil Taxonomy*, Science Press, Beijing.

IPCC (2007), Climate Change 2007: The Physical Science Basis, *Contribution of Working Group I to the Fourth Assessment Report of the Intergovernmental Panel on Climate Change*, edited by S. Solomon, D. Qin, and M. Manning, Cambridge Univ. Press, Cambridge, U. K.

Jung, M., G. Le Maire, S. Zaehle, S. Luyssaert, M. Vetter, G. Churkina, P. Ciais, N. Viovy, and M. Reichstein (2007), Assessing the ability of three land ecosystem models to simulate gross carbon uptake of forests from boreal to Mediterranean climate in Europe, *Biogeosciences*, *4*, 647–656.

Kato, T., Y. Tang, S. Gu, X. Cui, M. Hirota, M. Du, Y. Li, X. Zhao, and T. Oikawa (2004), Carbon dioxide exchange between the atmosphere and an alpine meadow ecosystem on the Qinghai-Tibetan Plateau, China, *Agric. For. Meteorol.*, *124*, 121–134, doi:10.1016/j.agrformet.2003.12.008.

Kato, T., Y. Tang, S. Gu, M. Hirota, M. Du, Y. Li, and X. Zhao (2006), Temperature and biomass influences on interannual changes in CO_2 exchange in an alpine meadow on the Qinghai-Tibetan Plateau, *Global Change Biol.*, *12*, 1285–1298, doi:10.1111/j.1365-2486.2006.01153.x.

Krinner, G., N. Viovy, N. de Noblet-Ducoudré, J. Ogée, J. Polcher, P. Friedlingstein, P. Ciais, S. Sitch, and I. C. Prentice (2005), A dynamic global vegetation model for studies of the coupled atmosphere-biosphere system, *Global Biogeochem. Cycles*, *19*, GB1015, doi:10.1029/2003GB002199.

Li, W., and X. Zhou (Eds.) (1998), *Ecosystems of Qingha-Xizang (Tibetan) Plateau and Approach for Their Sustainable Management*, pp. 1–2, Guangdong Sci. and Technol. Press, Guangzhou, China.

Li, Z., and Q. Zhao (2001), Organic carbon content and distribution in soils under different land uses in tropical and subtropical China, *Plant Soil*, *231*, 175–185, doi:10.1023/A:1010350020951.

Liu, X., and B. Chen (2000), Climatic warming in the Tibetan Plateau during recent decades, *Int. J. Climatol.*, *20*, 1729–1742, doi:10.1002/1097-0088(20001130)20:14<1729::AID-JOC556>3.0.CO;2-Y.

Liu, Y., Q. Bao, A. Duan, Z. Qian, and G. Wu (2007), Recent progress in the impact of the Tibetan Plateau on climate in China, *Adv. Atmos. Sci.*, *24*, 1060–1076, doi:10.1007/s00376-007-1060-3.

Mitchell, T. D., and P. D. Jones (2005), An improved method of constructing a database of monthly climate observations and associated high-resolution grids, *Int. J. Climatol.*, *25*, 693–712, doi:10.1002/joc.1181.

Myneni, R. B., R. R. Nemani, and S. W. Running (1997), Estimation of global leaf area index and absorbed par using radiative transfer models, *IEEE Trans. Geosci. Remote Sens.*, *35*, 1380–1393, doi:10.1109/36.649788.

National Soil Survey Office (Ed.) (1993), *Soil Species of China*, vol. 1, China Agric. Press, Beijing.

National Soil Survey Office (Ed.) (1994a), *Soil Species of China*, vol. 2, China Agric. Press, Beijing.

National Soil Survey Office (Ed.) (1994b), *Soil Species of China*, vol. 3, China Agric. Press, Beijing.

National Soil Survey Office (Ed.) (1995a), *Soil Species of China*, vol. 4, China Agric. Press, Beijing.

National Soil Survey Office (Ed.) (1995b), *Soil Species of China*, vol. 5, China Agric. Press, Beijing.

National Soil Survey Office (Ed.) (1996), *Soil Species of China*, vol. 6, China Agric. Press, Beijing.

National Soil Survey Office (Ed.) (1998), *Soils of China*, China Agric. Press, Beijing.

Niu, T., L. X. Chen, and Z. J. Zhou (2004), The characteristics of climate change over the Tibetan Plateau in the last 40 years and the detection of climatic jumps, *Adv. Atmos. Sci.*, *21*, 193–203, doi:10.1007/BF02915705.

Peng, S. S., S. L. Piao, T. Wang, J. Y. Sun, and Z. H. Shen (2009), Temperature sensitivity of soil respiration in different ecosystems in China, *Soil Biol. Biochem.*, doi:10.1016/j.soilbio.2008.10.023.

Piao, S. L., J. Y. Fang, and J. S. He (2006a), Variations in vegetation net primary production in the Qinghai-Xizang Plateau, China, from 1982 to 1999, *Clim. Change*, *74*, 253–267, doi:10.1007/s10584-005-6339-8.

Piao, S. L., P. Friedlingstein, P. Ciais, L. Zhou, and A. Chen (2006b), Effect of climate and CO_2 changes on the greening of the Northern Hemisphere over the past two decades, *Geophys. Res. Lett.*, *33*, L23402, doi:10.1029/2006GL028205.

Piao, S. L., J. Y. Fang, L. M. Zhou, K. Tan, and S. Tao (2007a), Changes in biomass carbon stocks in China's grasslands between 1982 and 1999, *Global Biogeochem. Cycles*, *21*, GB2002, doi:10.1029/2005GB002634.

Piao, S. L., P. Friedlingstein, P. Ciais, N. Viovy, and J. Demarty (2007b), Growing season extension and its effects on terrestrial carbon flux over the last two decades, *Global Biogeochem. Cycles*, *21*, GB3018, doi:10.1029/2006GB002888.

Piao, S. L., et al. (2008), Net carbon dioxide losses of northern ecosystems in response to autumn warming, *Nature*, *451*, 49–52, doi:10.1038/nature06444.

Piao, S., P. Ciais, P. Friedlingstein, N. de Noblet-Ducoudré, P. Cadule, N. Viovy, and T. Wang (2009), Spatiotemporal patterns of terrestrial carbon cycle during the 20th century, *Global Biogeochem. Cycles*, *23*, GB4026, doi:10.1029/2008GB003339.

Pinzon, J., M. E. Brown, and C. J. Tucker (2005), Satellite time series correction of orbital drift artifacts using empirical mode decomposition, in *Hilbert-Huang Transform: Introduction and Applications*, edited by N. Huang, pp. 167–186, World Sci. Press, Hackensack, N. J.

Post, W. M., W. R. Emanuel, P. J. Zinke, and A. G. Stangenberger (1982), Soil carbon pools and world life zones, *Nature*, *298*, 156–159, doi:10.1038/298156a0.

Santaren, D., P. Peylin, N. Viovy, and P. Ciais (2007), Optimizing a process-based ecosystem model with eddy-covariance flux measurements: A pine forest in southern France, *Global Biogeochem. Cycles*, *21*, GB2013, doi:10.1029/2006GB002834.

Scurlock, J. M. O., and D. O. Hall (1998), The global carbon sink: A grassland perspective, *Global Change Biol.*, *4*, 229–233, doi:10.1046/j.1365-2486.1998.00151.x.

Sitch, S., P. M. Cox, W. J. Collins, and C. Huntingford (2007), Indirect radiative forcing of climate change through ozone effects on the land-carbon sink, *Nature*, *448*, 791–794, doi:10.1038/nature06059.

Sun, H. L. (1996), *Formation and Evolution of the Qinghai-Xizang Plateau* (in Chinese), pp. 168–192, Shanghai Sci. and Technol. Press, Shanghai.

Tucker, C. J., J. E. Pinzon, M. E. Brown, D. Slayback, E. W. Pak, R. Mahoney, E. Vermote, and N. E. Saleous (2005), An Extended AVHRR 8-km NDVI Data Set Compatible with MODIS and SPOT Vegetation NDVI Data, *Int. J. Remote Sens.*, *26*, 4485–4498, doi:10.1080/01431160500168686.

Wang, J., T. Chang, P. Li, H. Cheng, and H. Fang (2008), Vegetation carbon reserve and its relationship with climatic factors of grassland system in Tibet (in Chinese), *J. Soil Water Conserv.*, *22*, 120–125.

Wang, S. Q., H. Q. Tian, J. Y. Liu, and S. F. Pan (2003), Pattern and change of soil organic carbon storage in China: 1960s–1980s, *Tellus, Ser. B*, *55*, 416–427, doi:10.1034/j.1600-0889.2003.00039.x.

Webb, E. K., G. I. Pearman, and R. Leuning (1980), Correction of flux measurements for density effects due to heat and water vapor transport, *Q. J. R. Meteorol. Soc.*, *106*, 85–100, doi:10.1002/qj.49710644707.

Wu, H. B., Z. T. Guo, and C. H. Peng (2003), Distribution and storage of soil organic carbon in China, *Global Biogeochem. Cycles*, *17*(2), 1048, doi:10.1029/2001GB001844.

Wutzler, T., and M. Reichstein (2008), Colimitation of decomposition by substrate and decomposers: A comparison of model formulations, *Biogeosciences*, *5*, 749–759.

Yang, Y. H., A. Mohammat, J. M. Feng, R. Zhou, and J. Y. Fang (2007), Storage, patterns and environmental controls of soil organic carbon in China, *Global Change Biol.*, *83*, 131–141.

Yang, Y. H., J. Y. Fang, Y. H. Tang, C. J. Ji, C. Y. Zheng, J. S. He, and B. Zhu (2008), Storage, patterns and controls of soil organic carbon in the Tibetan grasslands, *Biogeochemistry*, *13*, 1492–1499.

Zhang, Y. Q., Y. H. Tang, J. Jiang, and Y. H. Yang (2007), Characterizing the dynamics of soil organic carbon in grasslands on the Qinghai-Tibetan Plateau, *Sci. China Ser. D*, *50*, 113–120, doi:10.1007/s11430-007-2032-2.

Zheng, D., Q. S. Zhang, and S. H. Wu (2000), *Mountain Geoecology and Sustainable Development of the Tibetan Plateau*, 393 pp., Kluwer Acad., Norwell, Mass.

P. Ciais and N. Vuichard, UMR CEA, LSCE, CNRS, Bat. 709, CE, L'Orme des Merisiers, F-91191 Gif-sur-Yvette, France.

J. Fang, S. Liang, S. Piao, and K. Tan, Department of Ecology, College of Urban and Environmental Science, and Key Laboratory for Earth Surface Processes of the Ministry of Education, Peking University, Beijing 100871, China. (slpiao@pku.edu.cn)

Y. Tang, National Institute for Environmental Studies, Tsukuba, Ibaraki 305-8569, Japan.

X. Wu, Chinese Research Academy of Environmental Sciences, Beijing 100012, China.